Volume 50 | Number 64 | 18 August 2014 | Pages 8803–9016

ChemComm

Chemical Communications
www.rsc.org/chemcomm

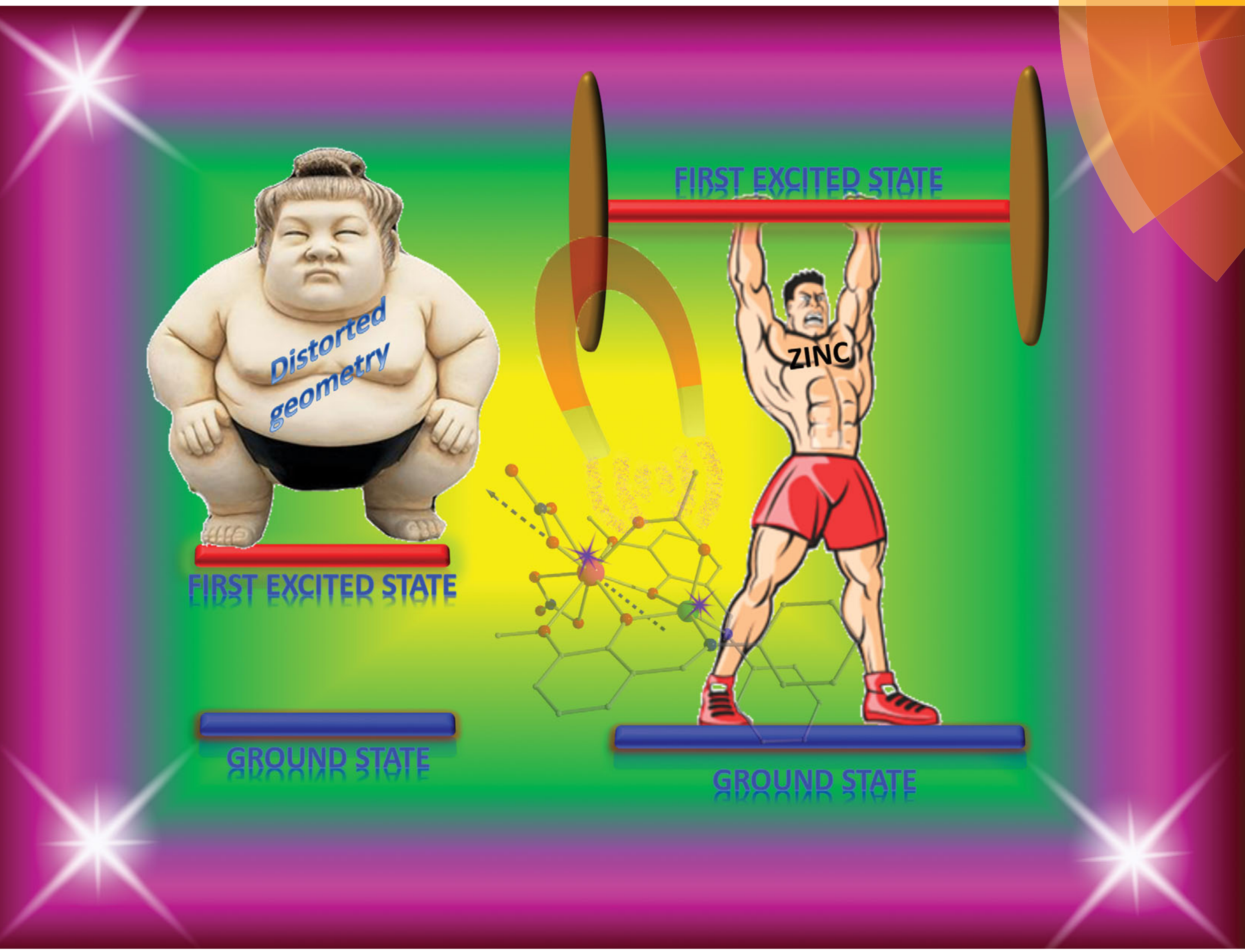

ISSN 1359-7345

ROYAL SOCIETY OF CHEMISTRY

COMMUNICATION
Gopalan Rajaraman, Maheswaran Shanmugam *et al.*
Enhancing the effective energy barrier of a Dy(III) SMM using a bridged diamagnetic Zn(II) ion

ChemComm

ROYAL SOCIETY OF CHEMISTRY

COMMUNICATION

View Article Online
View Journal | View Issue

Enhancing the effective energy barrier of a Dy(III) SMM using a bridged diamagnetic Zn(II) ion†

Cite this: *Chem. Commun.*, 2014, 50, 8838

Received 20th March 2014, Accepted 26th April 2014

DOI: 10.1039/c4cc02094d

www.rsc.org/chemcomm

Apoorva Upadhyay,[a] Saurabh Kumar Singh,[a] Chinmoy Das,[a] Ranajit Mondol,[a] Stuart K. Langley,[b] Keith S. Murray,[b] Gopalan Rajaraman*[a] and Maheswaran Shanmugam*[a]

Field induced single-molecule-magnet behaviour is observed for both a heterodinuclear $[ZnDy(L^-)_2]^{3+}$ complex (1) and a mononuclear $[Dy(HL)_2]^{3+}$ complex (2), with effective energy barriers of 83 cm^{-1} and 16 cm^{-1}, respectively. Insights into the relaxation mechanism(s) and barrier heights are provided via *ab initio* and DFT calculations. Our findings reveal an interesting observation that the U_{eff} of SMMs can be enhanced by incorporating diamagnetic metal ions.

Following the discovery, in 2003, that a terbium bis-phthalocyaninato($Tb(Pc)_2$) complex displays single molecule magnet (SMM) behaviour, a plethora of mononuclear and polynuclear lanthanide SMMs have since been reported.[1] Particular attention has been devoted to dysprosium(III) based SMMs, not only due to their fascinating magnetic behaviour, but also because of their interesting electronic, ferroelectric and luminescent properties.[2] Recent studies into mononuclear lanthanide SMMs have shown that only a select number of dysprosium(III) complexes display such behaviour in the absence of an applied magnetic field.[3] The majority, however, require the application of a magnetic field and are thus termed field induced SMMs. While significant experimental and theoretical efforts have been undertaken, a rational approach to enhance the barrier for the reorientation of magnetization (U_{eff}) is yet to be achieved. Of notable importance is recent work illustrating the effect of electron withdrawing groups on terminally coordinated ligands enabling fine tuning of the U_{eff} values.[4]

In this communication we present a synthetic strategy, without modification of the basal ligand architecture, showing a potential avenue towards the improvement of the U_{eff} parameter in lanthanide based SMMs, by incorporating a diamagnetic metal ion. Thus we have isolated and structurally characterised two novel compounds with formulae $[ZnDy(NO_3)_2(L)_2(CH_3CO_2)]$ (**1**) and $[Dy(HL)_2(NO_3)_3]$ (**2**), using the potentially binucleating Schiff base ligand 2-methoxy-6-[(*E*)-phenyliminomethyl]phenol (HL). We then place a particular focus, experimentally and theoretically, on their dynamic magnetic properties.

Single crystal X-ray diffraction reveals that **1** (Fig. 1A) crystallizes in the triclinic space group, $P\bar{1}$ (Table S1, ESI†), with the asymmetric unit containing the entire heterodinuclear complex consisting of one Dy^{III} and one Zn^{II} ion. The zinc ion present displays a distorted square pyramidal geometry with a $\{N_2O_2\}$ equatorial coordination sphere derived from the two deprotonated L^- ligands. The apical position is provided by an O-atom from the acetate ligand. The trivalent dysprosium ion shows a distorted tri-capped trigonal prismatic geometry, with a $\{DyO_9\}$ coordination sphere. Linkage between the Zn^{II} and Dy^{III} ions is provided by two phenoxo bridges and the carboxylate ligand, the latter displaying a μ–η^1–η^1 bonding mode. The methoxy group of the Schiff base ligand and the two chelating nitrate ions complete the coordination sphere of the Dy^{III} ion. Similar structures have recently been reported by several authors using compartmentalized Schiff base ligands.[2g,3a,5] Complex **2** crystallizes in the orthorhombic, space group, *Aba*2 (Table S1, ESI†). The asymmetric unit consists of two unique Dy^{III} mononuclear complexes, both containing two protonated ligands (HL) and three chelating nitrates. The two molecules differ from each other by the relative orientation of the ligands bound to the Dy^{III} ion. In the first complex, three chelating nitrate ions are oriented in a near trigonal planar arrangement, with the two Schiff base ligands, which chelate *via* the phenoxo and methoxy sites being perpendicular to the near trigonal plane of the nitrate ions (**2a**, see Fig. 1B). The second unique molecule, unlike in **2a**, has the HL ligands adjacent to each other, with the orientation of the chelating nitrates being distinctly different (**2b**, Fig. 1C). Complexes **2a** and **2b** are therefore found to be geometric isomers, crystallizing in the same crystal lattice. To the best of our knowledge, such isomerism for a lanthanide complex is observed here for the first time, although there is precedence for coordination isomers.[6] The Dy^{III} ions for both **2a** and **2b** are ten coordinate, displaying distorted bi-capped

[a] *Department of Chemistry, Indian Institute of Technology Bombay, Powai, Mumbai, Maharashtra, India-400076. E-mail: eswar@chem.iitb.ac.in, rajaraman@chem.iitb.ac.in; Fax: +91-22-2576-7152; Tel: +91-22-2576-7187*

[b] *School of Chemistry, Monash University, Clayton, Victoria 3800, Australia*

† Electronic supplementary information (ESI) available: CIF files for **1** and **2**, *M vs. H*, Cole–Cole plots, figures and tables corresponding to the spin density and Kramers doublet energies for **1** and **2**, along with other reported Dy/DyZn complexes. CCDC 990256 and 990257. For ESI and crystallographic data in CIF or other electronic format see DOI: 10.1039/c4cc02094d

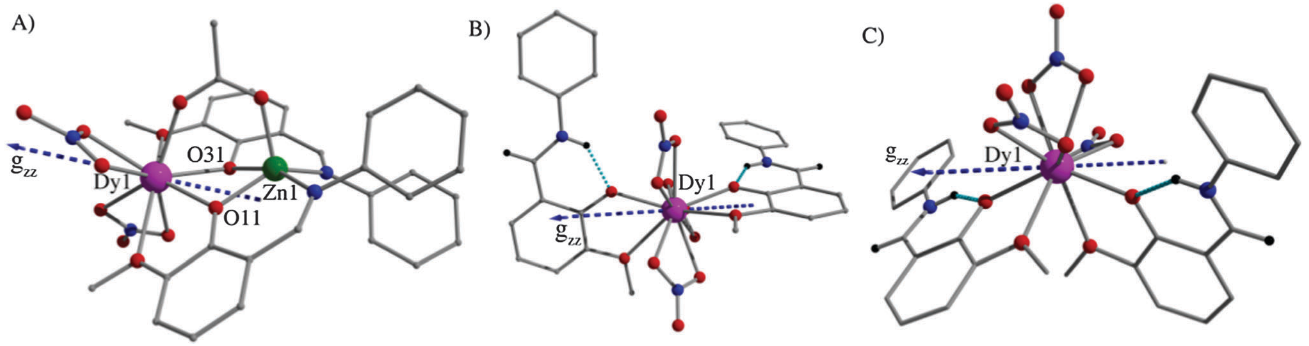

Fig. 1 (A) Ball and stick representations of the molecular structures of (A) **1**, (B) **2a** and (C) **2b**, the hydrogen atoms are removed for clarity. The blue arrow represents the computed easy axis anisotropy. The sky blue dotted bonds in (B) and (C) represent the intramolecular hydrogen bonding between imine proton and phenolic oxygen of the ligand. Colour code: magenta = Dy(III), green = Zn(II); red = O; blue = N; grey = C; black = H.

square anti-prismatic geometries, with $\{DyO_{10}\}$ coordination spheres. It is also observed that the phenolic proton attached to the free ligand migrates to the imino (–C=N) when complexed to the metal. Such a scenario has been witnessed in other reported lanthanide complexes.[7] The nitrate groups in **1** and **2** facilitate intermolecular hydrogen bonding interactions (Fig. S1, ESI†). Selected bond lengths and angles are given in Table S2 (ESI†).

Direct current (dc) magnetic susceptibility measurements on polycrystalline samples of **1** and **2** were carried out at an applied magnetic field of 1.0 T in the 1.8–300 K temperature range (Fig. 2). The observed room temperature $\chi_M T$ values of 14.10 cm^3 K mol^{-1} and 14.06 cm^3 K mol^{-1} for **1** and **2**, respectively, are in good agreement with the expected value of 14.17 cm^3 K mol^{-1} for a mononuclear dysprosium(III) ion ($^6H_{15/2}$; $g = 4/3$). Upon reducing the temperature, a gradual decrease in $\chi_M T$ is observed for both **1** and **2** up to $\sim$60 K, before falling more rapidly below this temperature. These decreases are a result of the anisotropy associated with both

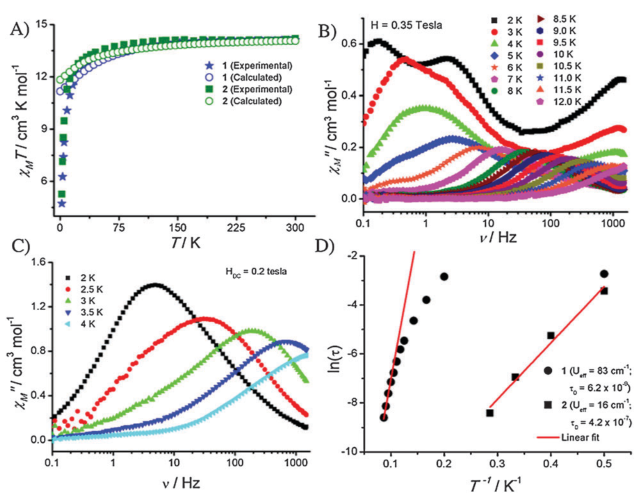

Fig. 2 (A) Temperature dependent magnetic susceptibility plot for **1** and **2** with an applied field of 1.0 T. The *ab initio* calculated values for **1** (blue) and **2** (green) shown as open circles. (B) and (C) Frequency dependent out-of-phase susceptibility plots for **1** (2.0 to 12 K) and **2** (2.0 to 4.0 K) at the indicated optimum external magnetic field. (D) Arrhenius plot constructed from the ac data of **1** (filled circle) and **2** (filled square).

the complexes, however contributions from intermolecular antiferromagnetic or dipolar interactions cannot be ruled out. A steep increase is then observed in the isothermal magnetization *versus* field plots at low temperature and fields. At larger magnetic fields the magnetization displays a linear response, without any clear saturation of the curve. The non-superimposable nature of the reduced magnetization plots (Fig. S2, ESI†) further reiterates the existence of strong magnetic anisotropy associated with both **1** and **2**.

In order to study the magnetic relaxation dynamics of **1** and **2**, variable temperature and frequency dependent alternating current (ac) susceptibility measurements were performed on polycrystalline samples, in both zero and applied external dc magnetic fields. Upon using a 3.5 Oe oscillating ac field, with a zero dc field, an absence of any frequency dependent out-of-phase susceptibility (χ_M'') signals for both **1** and **2** indicates no significant blockage of the magnetization, above 1.8 K. This observation is found in the majority of mononuclear Dy^{III} complexes and is ascribed to fast QTM.[2a,d,8] Upon application of a static dc magnetic field, however, temperature and frequency dependent χ_M'' signals are observed for both **1** (Fig. 2B) and **2** (Fig. 2C). This is a clear indication of slow magnetic relaxation occurring in these complexes, a characteristic signature of a SMM. It was found that the optimum dc magnetic fields, where the relaxation is slowest, are found to be 0.35 T and 0.2 T, for **1** and **2**, respectively, and a full frequency and temperature analysis was performed at these fields. Analysis of the isothermal χ_M'' *versus* frequency plot, for **1**, shows multiple relaxation pathways which are particularly visible at the lowest temperatures, with three frequency dependent maxima observed at 1.8 K (Fig. S3, ESI†). For complex **2** (where two different geometric isomers **2a** and **2b** are found in the crystal), we observe one predominant maximum in the χ_M'' *versus* frequency plot, indicative of a single relaxation process (Fig. 2C). The Cole–Cole plot, however, suggests that multiple relaxation processes are in operation (Fig. S3D, ESI†). Observation of these multiple relaxation processes in **1** and **2** has been rationalized by *ab initio* calculations (*vide infra*). The relaxation follows a thermally activated mechanism above 10 and 2 K for **1** and **2**, respectively, and plots of ln(τ) *vs.* 1/T are linear. Fitting the activated relaxation data to the Arrhenius law [$\tau = \tau_0 \exp(U_{eff}/k_B T)$] yields effective energy barriers of 83 cm^{-1} and 16 cm^{-1}, with $\tau_0 = 6.2 \times 10^{-9}$ s and 4.2×10^{-7} s for **1** and **2**, respectively (Fig. 2D).

In an attempt to rationalize the fivefold increase of the energy barrier for **1** compared to **2**, *ab initio* calculations were performed using the MOLCAS 7.8 code.[9] The computed electronic and magnetic properties show that the local *g*-tensors in the ground Kramers doublet in **1** have the values of [g_{xx} = 0.02, g_{yy} = 0.04 and g_{zz} = 18.82], while the *g*-tensors for **2a** and **2b** are computed to be [g_{xx} = 0.020, g_{yy} = 0.036, g_{zz} = 19.443] and [g_{xx} = 0.081, g_{yy} = 0.121, g_{zz} = 19.092], respectively (see Tables S3–S5, ESI†). All the computed *g* anisotropies are strongly axial in nature (see Fig. 1 for computed g_{zz} orientation, see also Fig. S4–S6 of ESI†) but are not of pure Ising type. The computed energies of the first excited Kramers doublet, which often correlates to the height of the energy barrier (U_{eff}) in lanthanide single ion magnets, is found to be 91 cm^{-1} for **1**, and 76 cm^{-1} and 46 cm^{-1} for **2a** and **2b**, respectively. A drastic variation in the ground-state to first-excited state gap suggests that this separation is extremely sensitive to small structural changes. The value obtained for **1** is in close agreement with the experimental results, while for **2** the values are overestimated. As shown in Fig. 2A the calculated temperature dependent susceptibility and magnetization data for **1** and **2a**/**2b** are in good agreement with the experimental data (ESI,† Fig. S7 and S8), this encouraged us to probe the mechanism(s) of relaxation in **1** and **2a**/**b**, using these parameters (see Fig. 3 and Fig. S9 (for **2b**)). For both complexes, QTM *via* the ground state is expected, and this is corroborated experimentally through the absence of SMM behaviour in the zero dc field. The applied dc field lifts the degeneracy of Kramers doublets and quenches the QTM to a certain extent, while thermally assisted QTM and an Orbach relaxation process are activated *via* the first excited state as the principal magnetization axis does not coincide with the ground state (see Tables S3–S5 of ESI†). The computed matrix elements between the connecting pairs could possibly account for the observed multiple relaxations in **1** and **2**. It should be noted that the probability of QTM *via* the ground state is predicted to be slightly higher in the case of complex **1** due to the reduced axiality of the ground Kramers doublet, when compared to **2a** and **2b** (Fig. 3). From Fig. 3 (and Fig. S9, ESI†) it is also apparent that **2a** and **2b** have ±13/2 as the first excited state level (m_J = ±13/2; g_{xx} = 0.044, g_{yy} = 0.094, g_{zz} = 16.414),[1b,10] while the first excited state in **1** is highly transverse in nature, (g_{xx} = 11.158, g_{yy} = 6.774, g_{zz} = 1.284),

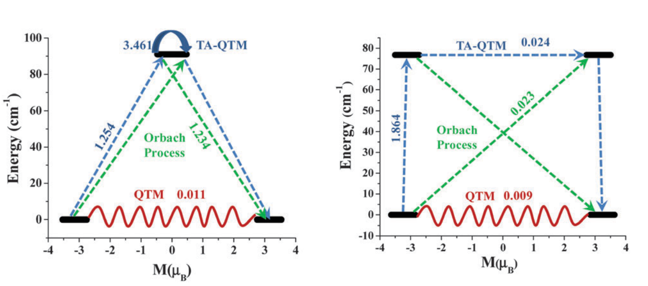

Fig. 3 *Ab initio* computed matrix elements between the connecting pairs (ground state and first excited state) in complex **1** (left) and complex **2a** (right). The thick black line indicates the Kramers doublets (KDs) as a function of magnetic moment. The dotted green lines show the possible pathway of the Orbach process. The zig–zag lines connecting the ground state KDs represent the QTM. The dotted blues lines show the thermally activated-QTM *via* the first excited state.

with a very small |μL_z| value (0.309), suggesting the presence of an m_J = 1/2 state (see Tables S3–S6, ESI†). The observed change in the electronic structure of the Stark levels in **1** could be due to structural distortions/presence of a low symmetry environment, which are the likely cause for the stabilization of the m_J = 1/2 state over other Kramers levels with larger m_J values.

Because of this change, the mechanism of relaxation is expected to be drastically different with thermally activated-QTM being the dominant process for **1** as the excited level has significant transverse anisotropy while TA-QTM–Orbach relaxation are operative for **2**.[11] This is supported by the tentative mechanism derived from the *ab initio* calculations (Fig. 3).

As it was shown experimentally that **1** displays a larger U_{eff} value than **2** we now turn to analyse the role, if any, the Zn^{II} ions play towards this observation. DFT calculations reveal that the bridging phenoxo oxygen atoms in **1** have higher negative charges compared to that of the coordinated oxygen atom in **2** (−0.73 *vs.* −0.3, see Fig. S10–S12 of ESI† and also Tables S7–S9, ESI†). The presence of a dicationic Zn^{II} ion leads to a larger charge polarization on the oxygen atom, which in turn induces a large electrostatic interaction on the lanthanide ions. This eventually leads to the destabilization of excited states and therefore an increased ground-state to first-excited state gap. This strongly suggests that the presence of a cation near the coordination environment is likely to help and enhance the U_{eff} barrier. This has been witnessed earlier in Na[Dy(DOTA)] and {Dy_4K_2} clusters.[1b,12] This point is validated further by the fact that all the reported {ZnDy} molecules have higher U_{eff} than the monomeric {Dy} analogues (see Tables S10 and S11 of ESI†). We have also extended our calculations to selected complexes which are structurally related to **1** (Table S10 and Fig. S13, ESI†) to reiterate this point (increased U_{eff}) and have also sought correlation of computed U_{eff} values to specific structural parameters. The large discrepancy in U_{eff} among the structurally related Zn–Dy complexes (similar to **1**) are found to correlate with the deviation calculated from the ideal tricapped trigonal prism geometry using the continuous shape measurement methodology (see Fig. S14 of ESI†).[13] The lower deviations from the ideal structures are found to yield larger U_{eff} values. Since the electrostatic repulsion is expected to be significant for an idealistic structure, the structural distortions are likely to lower the barrier (see ESI,† Table S10 for details).

In summary, the study sheds light on one of the long standing questions as to why zinc containing dysprosium complexes display enhanced SMM properties, over that of pure dysprosium complexes themselves. Evidence of large U_{eff} values in complexes containing other diamagnetic ions such as Co^{III} has also been reported.[6,14] Based on our calculations, we propose a new methodology to increase the magnetization relaxation barrier by simply incorporating diamagnetic ions along with anisotropic Dy(III) ions, a method that differs from other existing approaches.[4,15]

MS and GR wishes to thank the funding agencies DST (SR/S1/IC-32/2011; SR/S1/IC-41/2010), DST nanomission (SR/NM/NS-1119/2011) and IIT Bombay for financial support. GR and KSM acknowledge the support of an Australia–India AISRF grant. MS and GR wish to thank Professor L. Chibotaru for the MOLCAS code. We thank Dr B. Moubaraki for experimental assistance.

Notes and references

1 (*a*) N. Ishikawa, M. Sugita, T. Ishikawa, S.-Y. Koshihara and Y. Kaizu, *J. Am. Chem. Soc.*, 2003, **125**, 8694; (*b*) R. J. Blagg, L. Ungur, F. Tuna, J. Speak, P. Comar, D. Collison, W. Wernsdorfer, E. J. L. McInnes, L. F. Chibotaru and R. E. P. Winpenny, *Nat. Chem.*, 2013, **5**, 673; (*c*) N. F. Chilton, D. Collison, E. J. McInnes, R. E. Winpenny and A. Soncini, *Nat. Commun.*, 2013, **4**, 2551.

2 (*a*) D. N. Woodruff, R. E. P. Winpenny and R. A. Layfield, *Chem. Rev.*, 2013, **113**, 5110; (*b*) J. Ruiz, A. J. Mota, A. Rodriguez-Dieguez, S. Titos, J. M. Herrera, E. Ruiz, E. Cremades, J. P. Costes and E. Colacio, *Chem. Commun.*, 2012, **48**, 7916; (*c*) D. Aravena and E. Ruiz, *Inorg. Chem.*, 2013, **52**, 13770; (*d*) P. Zhang, L. Zhang and J. Tang, *Curr. Inorg. Chem.*, 2013, **3**, 101; (*e*) J. Luzon and R. Sessoli, *Dalton Trans.*, 2012, **41**, 13556; (*f*) X. Yi, K. Bernot, F. Pointillart, G. Poneti, G. Calvez, C. Daiguebonne, O. Guillou and R. Sessoli, *Chem. – Eur. J.*, 2012, **18**, 11379; (*g*) M. A. Palacios, S. Titos-Padilla, J. Ruiz, J. M. Herrera, S. J. A. Pope, E. K. Brechin and E. Colacio, *Inorg. Chem.*, 2014, **53**, 1465.

3 (*a*) A. Watanabe, A. Yamashita, M. Nakano, T. Yamamura and T. Kajiwara, *Chem. – Eur. J.*, 2011, **17**, 7428; (*b*) N. F. Chilton, S. K. Langley, B. Moubaraki, A. Soncini, S. R. Batten and K. S. Murray, *Chem. Sci.*, 2013, **4**, 1719–1730.

4 F. Habib, G. Brunet, V. Vieru, I. Korobkov, L. F. Chibotaru and M. Murugesu, *J. Am. Chem. Soc.*, 2013, **135**, 13242.

5 (*a*) K. Ehama, Y. Ohmichi, S. Sakamoto, T. Fujinami, N. Matsumoto, N. Mochida, T. Ishida, Y. Sunatsuki, M. Tsuchimoto and N. Re, *Inorg. Chem.*, 2013, **52**, 12828; (*b*) E. Colacio, J. Ruiz-Sanchez, F. J. White and E. K. Brechin, *Inorg. Chem.*, 2011, **50**, 7268; (*c*) P. Zhang, L. Zhang, S.-Y. Lin and J. Tang, *Inorg. Chem.*, 2013, **52**, 6595; (*d*) V. Chandrasekhar, A. Chakraborty and E. C. Sanudo, *Dalton Trans.*, 2013, **42**, 13436.

6 S. K. Langley, N. F. Chilton, L. Ungur, B. Moubaraki, L. F. Chibotaru and K. S. Murray, *Inorg. Chem.*, 2012, **51**, 11873.

7 (*a*) A. Upadhyay, S. Vaidya, V. S. Venkatasai, P. Jayapal, A. K. Srivastava, M. Shanmugam and M. Shanmugam, *Polyhedron*, 2013, **66**, 87; (*b*) J.-P. Costes, F. Dahan and F. Nicodeme, *Inorg. Chem.*, 2003, **42**, 6556; (*c*) W. Xie, M. J. Heeg and P. G. Wang, *Inorg. Chem.*, 1999, **38**, 2541.

8 (*a*) P. Zhang, Y.-N. Guo and J. Tang, *Coord. Chem. Rev.*, 2013, **257**, 1728; (*b*) P.-H. Lin, I. Korobkov, T. J. Burchell and M. Murugesu, *Dalton Trans.*, 2012, **41**, 13649.

9 F. Aquilante, L. De Vico, N. Ferré, G. Ghigo, P.-å. Malmqvist, P. Neogrády, T. B. Pedersen, M. Pitoňák, M. Reiher, B. O. Roos, L. Serrano-Andrés, M. Urban, V. Veryazov and R. Lindh, *J. Comput. Chem.*, 2010, **31**, 224–247.

10 (*a*) L. Ungur and L. F. Chibotaru, *Phys. Chem. Chem. Phys.*, 2011, **13**, 20086; (*b*) L. Ungur, W. Van den Heuvel and L. F. Chibotaru, *New J. Chem.*, 2009, **33**, 1224; (*c*) L. F. Chibotaru, L. Ungur and A. Soncini, *Angew. Chem., Int. Ed.*, 2008, **47**, 4126.

11 Although Raman and Orbach processes are not determined directly by the matrix elements of the magnetic moments, the non-negligible values of the latter serve as an indicator of the relevance of these relaxation processes.

12 (*a*) M.-E. Boulon, G. Cucinotta, J. Luzon, C. Degl'Innocenti, M. Perfetti, K. Bernot, G. Calvez, A. Caneschi and R. Sessoli, *Angew. Chem., Int. Ed.*, 2013, **52**, 350–354; (*b*) G. Cucinotta, M. Perfetti, J. Luzon, M. Etienne, P.-E. Car, A. Caneschi, G. Calvez, K. Bernot and R. Sessoli, *Angew. Chem., Int. Ed.*, 2012, **51**, 1606; (*c*) J.-L. Liu, Y.-C. Chen, Y.-Z. Zheng, W.-Q. Lin, L. Ungur, W. Wernsdorfer, L. F. Chibotaru and M.-L. Tong, *Chem. Sci.*, 2013, **4**, 3310.

13 (*a*) H. Zabrodsky, S. Peleg and D. Avnir, *J. Am. Chem. Soc.*, 1992, **114**, 7843; (*b*) D. Anvir, O. Katzenelson, S. Keinan, M. Pinsky, Y. Pinto, Y. Salomon and H. Zabrodsky Hel-Or, *CSM: Conceptual Aspects*, England, 1997.

14 S. K. Langley, N. F. Chilton, B. Moubaraki and K. S. Murray, *Chem. Commun.*, 2013, **49**, 6965.

15 (*a*) S. Takamatsu, T. Ishikawa, S.-y. Koshihara and N. Ishikawa, *Inorg. Chem.*, 2007, **46**, 7250; (*b*) A. Baniodeh, V. Mereacre, N. Magnani, Y. Lan, J. A. Wolny, V. Schuenemann, C. E. Anson and A. K. Powell, *Chem. Commun.*, 2013, **49**, 9666; (*c*) J. D. Rinehart, M. Fang, W. J. Evans and J. R. Long, *Nat. Chem.*, 2011, **3**, 538; (*d*) J. D. Rinehart, M. Fang, W. J. Evans and J. R. Long, *J. Am. Chem. Soc.*, 2011, **133**, 14236.